Supplementary Information for:

Mechanistic insights into the enhancement or inhibition of phase separation by polyubiquitin chains of different lengths or linkages

Thuy P. Dao[1,#], Yiran Yang[2,#], Michael S. Cosgrove[3], Jesse B. Hopkins[4], Weikang Ma[4], Carlos A. Castañeda[1,5]

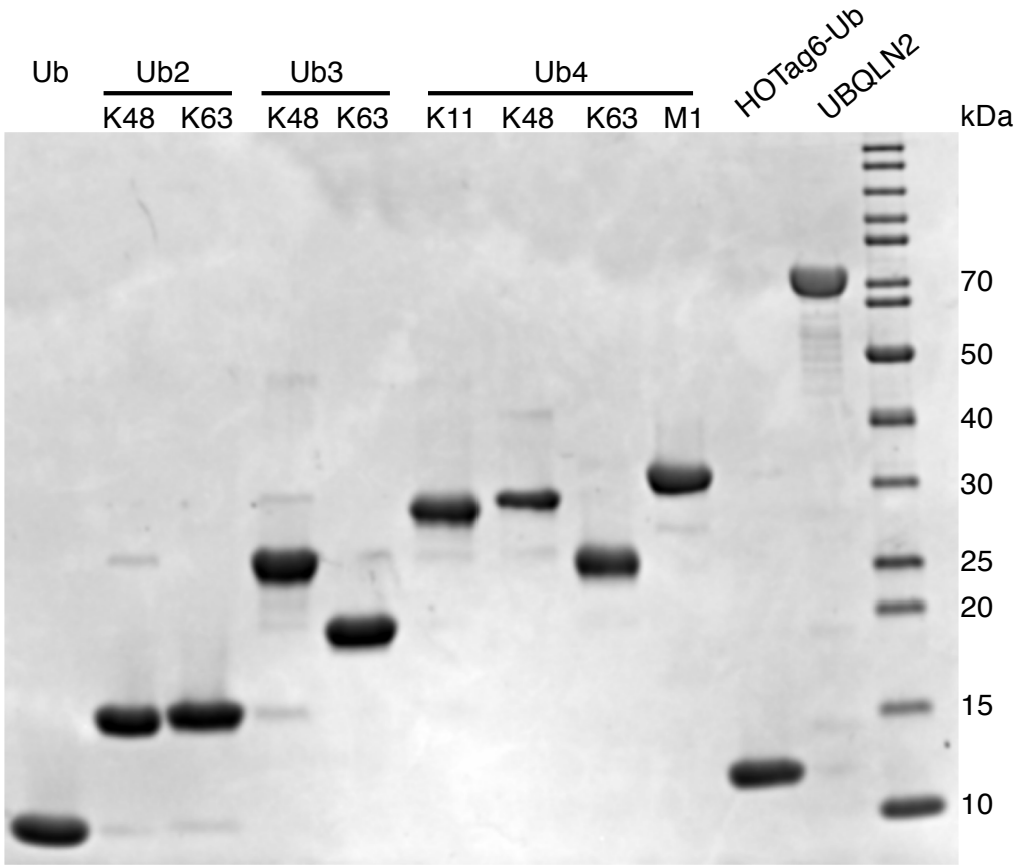

Supplementary Figure S1. SDS-PAGE gel of polyUb chains and UBQLN2 used in this study.

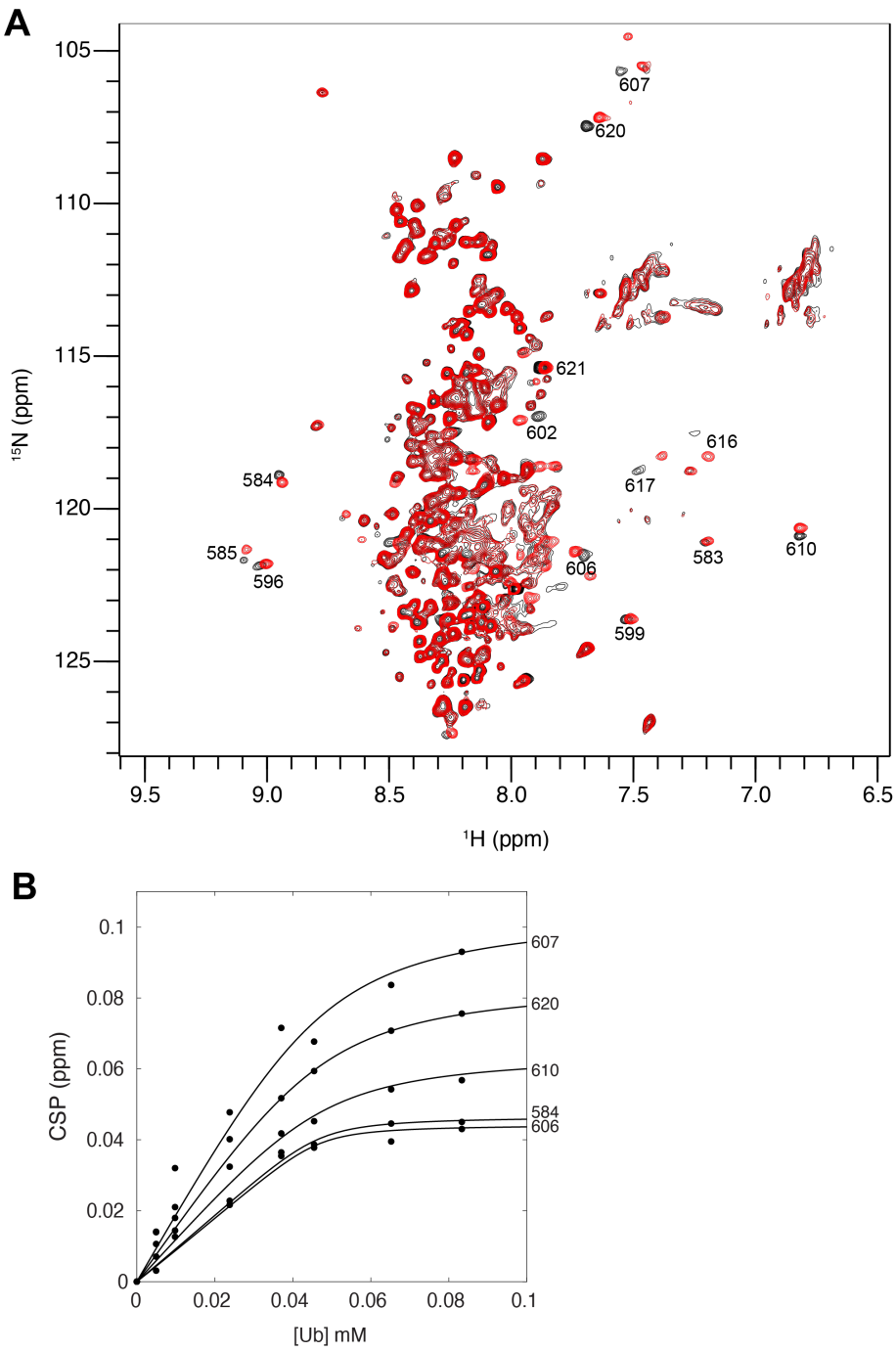

Supplementary Figure S2. (A) ^{15}N-^{1}H TROSY-HSQC spectra of FL UBQLN2 (50 μM) in the absence and presence of Ub (~2:1 Ub:UBQLN2 ratio). Highlighted are those amide resonances in the UBA that exhibited CSPs in the presence of Ub. These same residues are also involved in the self-interactions that are important for UBQLN2 LLPS. Spectra acquired and processed with identical parameters. (B) Residue-specific amide titration curves of UBQLN2. Fits from a single-site binding model were overlaid on experimental data points (K_d ~ 3 μM +/- 2 μM).

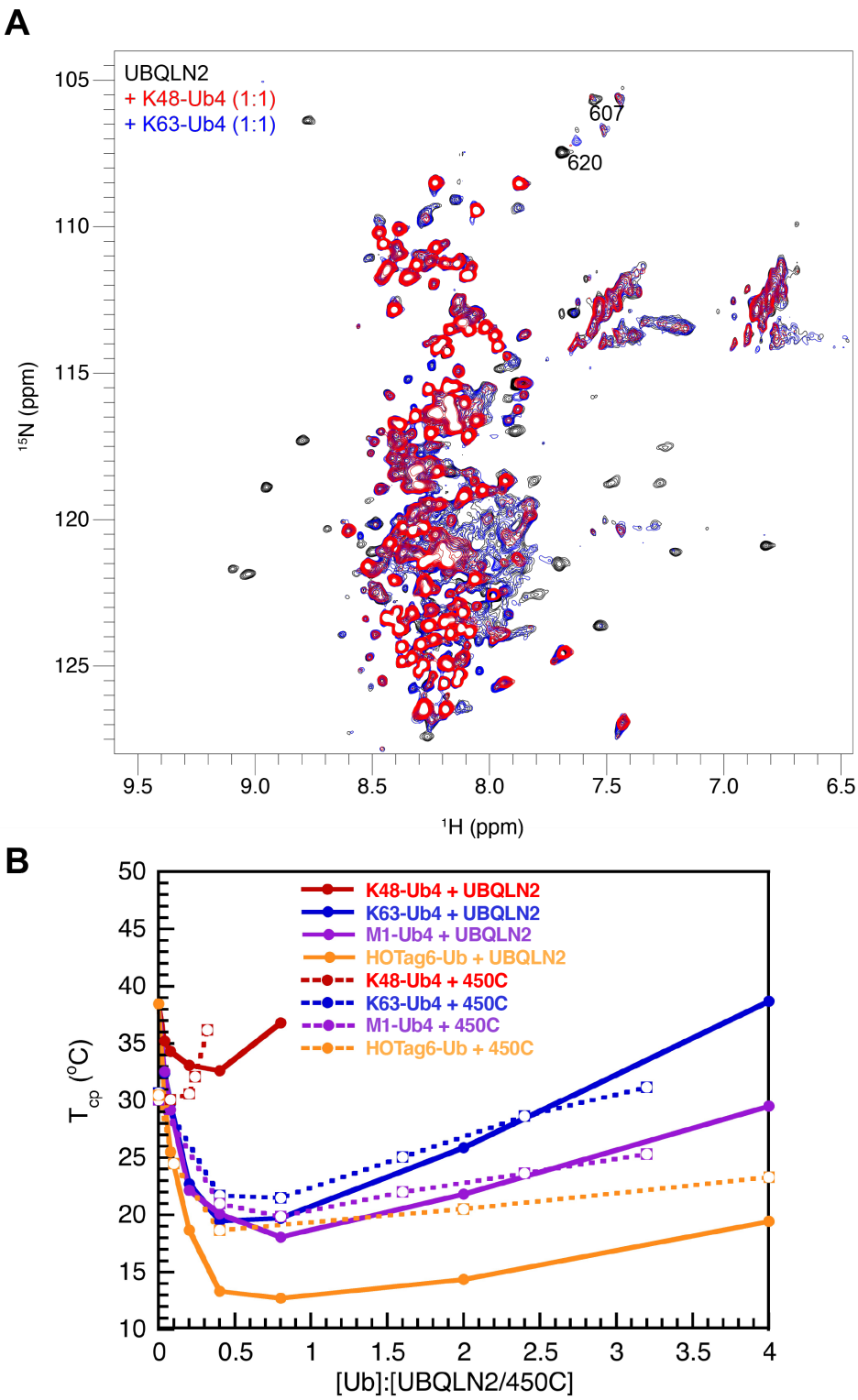

Supplementary Figure S3. (A) ^{15}N-^{1}H TROSY-HSQC spectra of FL UBQLN2 (50 μM) in the absence and presence of K48-Ub4 or K63-Ub4 (~1:1 Ub4:UBQLN2 ratio) as noted in the color legend. Note that UBA resonances are no longer visible upon addition of Ub4. Spectra acquired

and processed with identical parameters. (B) Temperature-composition phase diagram of FL UBQLN2 (at 30 μM) and UBQLN2 450-624 (at 100 μM) indicating that these two proteins are affected similarly by the addition of four different Ub4 chains. Using solutions containing distinct amounts of polyUb chain mixed with UBQLN2, the temperature midpoint of the phase transitions (cloud point temperatures (T_{cp})) were extracted from spectrophotometric turbidity assays as described in Methods. Solid and dashed line indicates the phase boundary of FL UBQLN2 and UBQLN2 450-624, respectively. Above this line, the solution is phase-separated, and below which the solution is homogeneous.

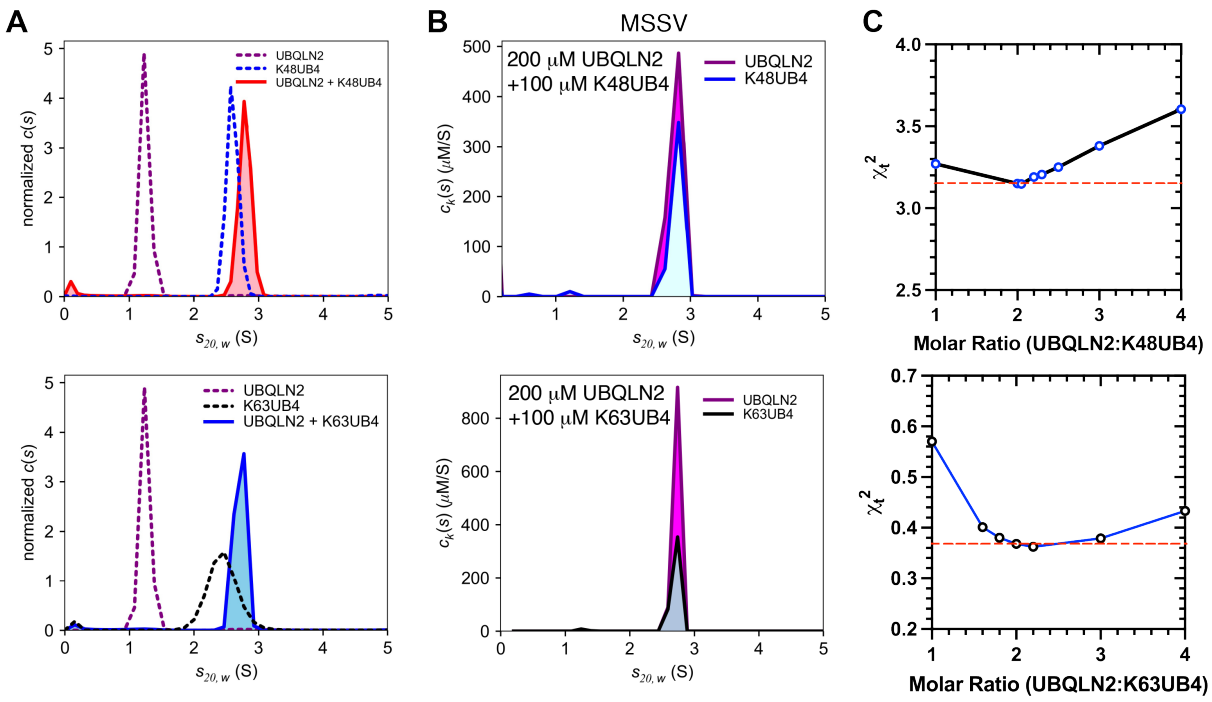

Supplementary Figure S4. Sedimentation velocity analytical ultracentrifugation (SV-AUC) experiments of UBQLN2 487-624 in the absence and presence of K48-Ub4 or K63-Ub4. (A) Normalized c(s) distribution for the individual components UBQLN2 487-624 (200 μM) and Ub4 (100 μM), as well as the UBQLN2:Ub4 complex at a loading stoichiometric ratio of 2:1 (this corresponds to a UBQLN2:Ub ratio of 1:2). (B, C) Multi-signal sedimentation velocity (MSSV) analysis to determine stoichiometry of UBQLN2:Ub4 complex with 200 μM UBQLN2 and 100 μM Ub4 (see Tables S3 and S4). Component $c_k(s)$ distributions for UBQLN2 and Ub4 are colored according to legend. No free UBQLN2 is observed in the $c_k(s)$ distribution for either complex. (C) To probe accuracy of calculated stoichiometry of the complex (Table S3), preconstrained values of the molar ratio were tested, and best fit (χ_t^2) values were determined. Experiments show best fit when molar ratio was constrained to an average of two UBQLN2 molecules bound for every Ub4 molecule.

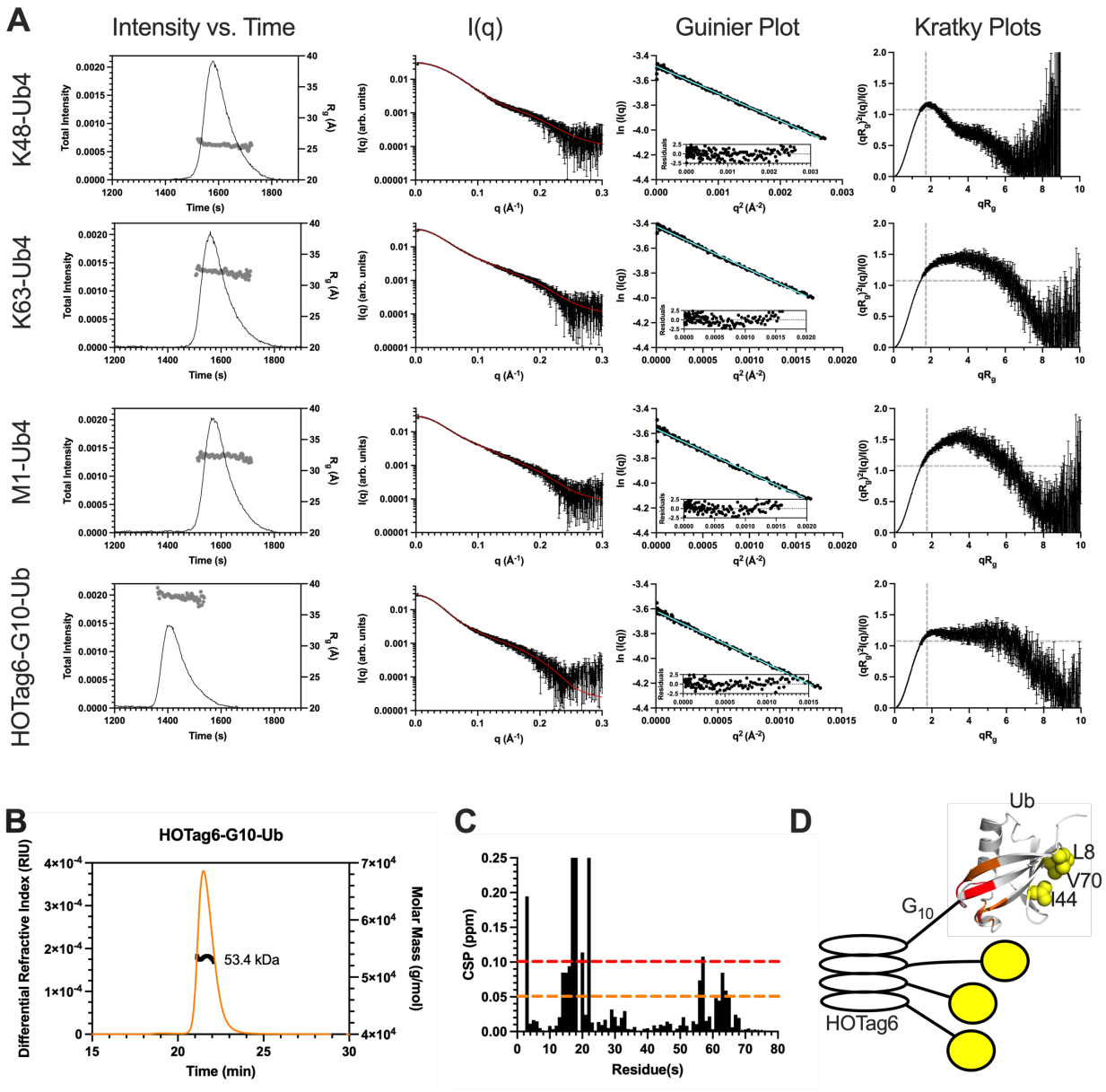

Supplementary Figure S5. (A) SEC-SAXS profiles for K48-Ub4, K63-Ub4, M1-Ub4, and HOTag6-G10-Ub. I(q) vs. q scattering curves (middle left) determined from frames 784-808 (K48-Ub4), 766-791 (K63-Ub4), 791-813 (M1-Ub4), and 705-728 (HOTag6-G10-Ub) on the corresponding SEC-SAXS profiles (left). Red line in I(q) profile indicates fit from P(r) analysis (see Fig. 4B). Cyan line in Guinier plot (middle right) is linear fit of ln(I(q)) vs. q^2, while inset shows residuals of fit. Dimensionless Kratky plots (right) include dashed lines to indicate where a globular protein would peak. Increase in polyUb chain flexibility from top (K48-Ub4) to bottom (HOTag6-G10-Ub) is indicated by shifts in the peak position up and to the right of the globular peak and larger plateaus in the higher q region. (B) HOTag6-G10-Ub is a tetramer; the

molecular weight (MW) of HOTag6-G10-Ub was determined using SEC-MALS-SAXS experiments. The observed MW value of 53.4 kDa is consistent with the expected MW of a HOTag6-G10-Ub tetramer (52.976 kDa), four times that of the monomer (13.244 kDa). (C) CSPs of amide resonances in the Ub unit of HOTag6-G10-Ub vs. monoUb. Note that no significant CSPs exist for the hydrophobic patch region consisting of residues 8, 44, and 70. (D) CSPs from panel B are mapped onto a cartoon model of the HOTag6-G10-Ub tetramer. CSPs are color-coded red (CSPs ≥ 0.1 ppm) and orange (CSPs ≥ 0.05 ppm). Hydrophobic patch residues 8, 44, and 70 are shown in sphere representation.

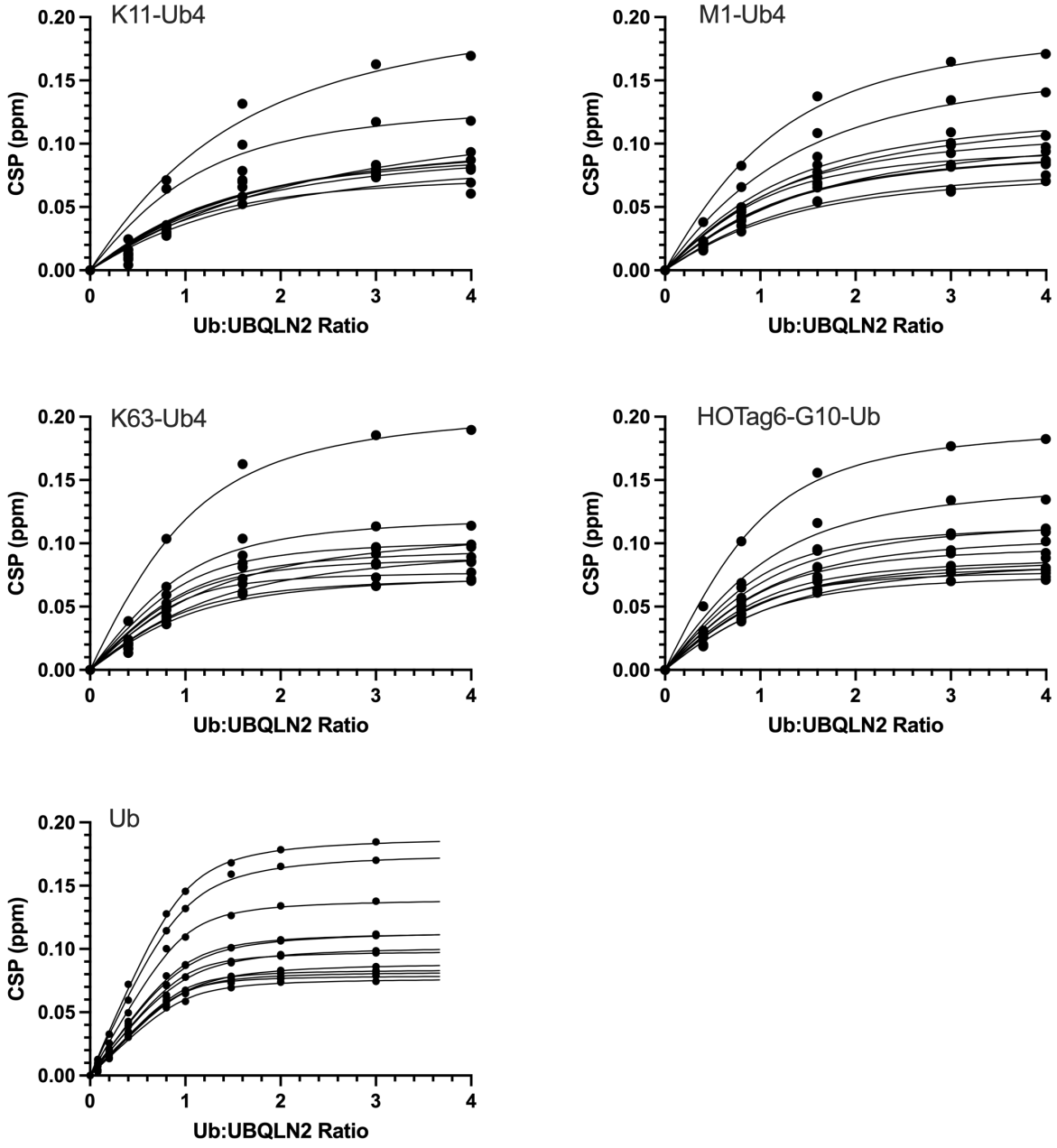

Supplementary Figure S6. UBQLN2 450-624 residue-specific titration curves in the presence of Ub or Ub4 as a function of Ub:UBQLN2 ratio. CSPs are weighted amide chemical shifts (see Methods). Data points are represented as circles with fit to single-site binding model (see Methods) shown as a line.

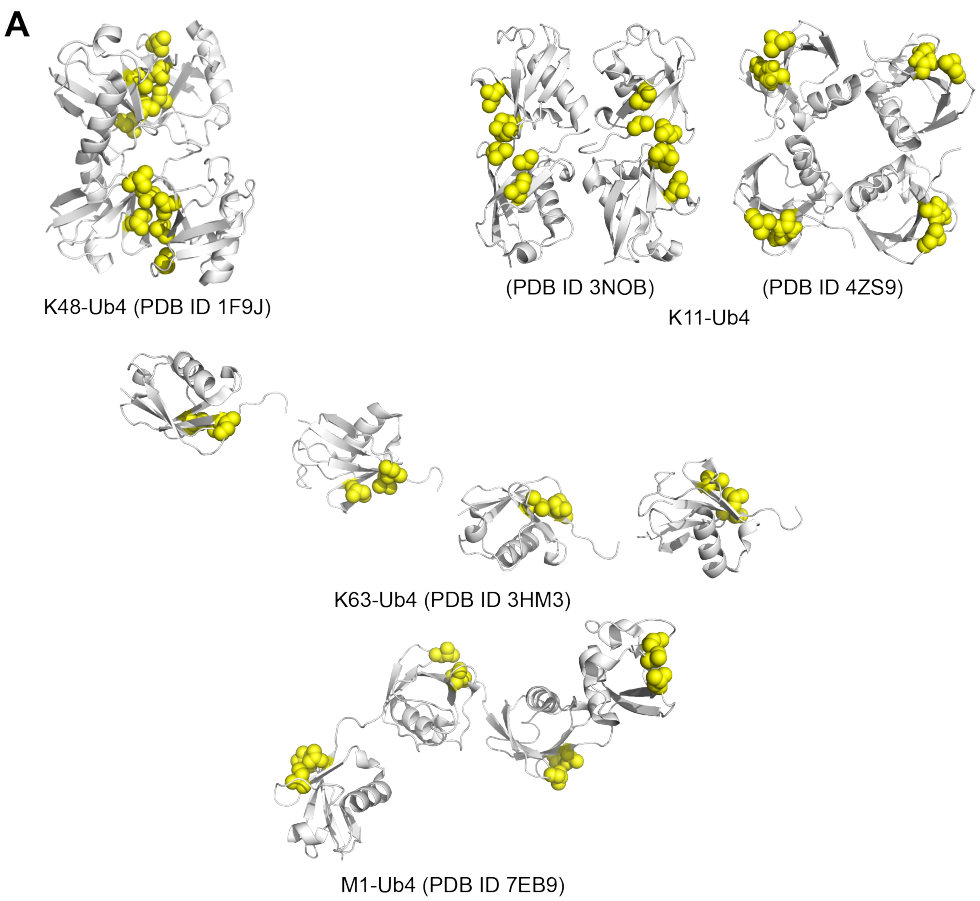

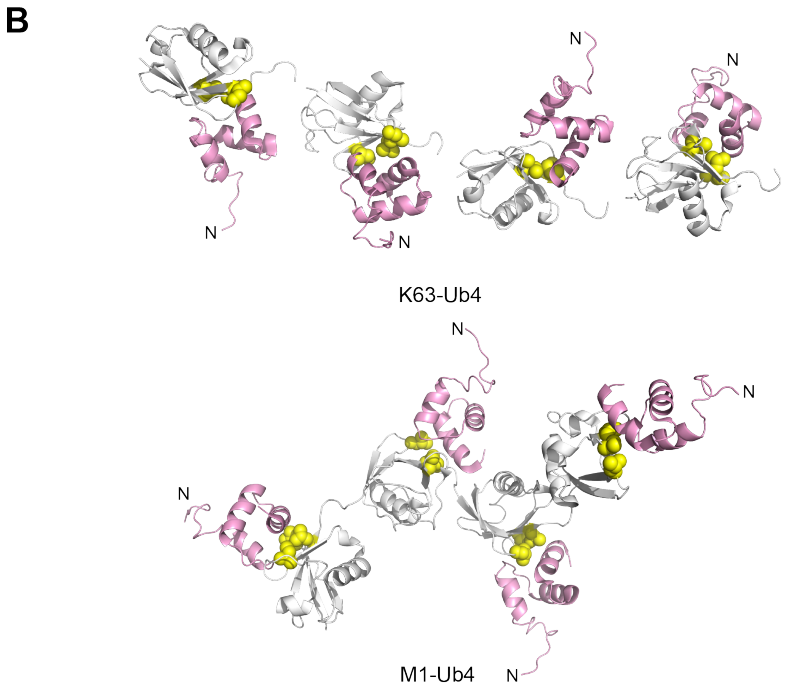

Supplementary Figure S7. (A) Representative structures of polyUb tetramers for K48-Ub4, K63-Ub4 and M1-Ub4 (with ligand removed) from PDB entries as noted. Shown are two putative

structures of K11-Ub4, based on K11-Ub2 (PDB ID 3NOB) or a model of K11-Ub4 (PDB ID 4Z9S, (Levin-Kravets et al., 2015)) based on K11-Ub2 in PDB ID 2XEW. Shown as yellow spheres are the hydrophobic patch residues L8, I44, and V70 in each Ub unit. Note the compact conformations of both K11-Ub4 and K48-Ub4, but extended conformations for M1-Ub4 and K63-Ub4. (B) Models of how UBQLN2 UBA domains (pink) could dock to either K63-linked or M1-linked polyUb chains. C-terminal UBQLN2 UBA domains were positioned by overlaying the UBQLN1 UBA:Ub complex from PDB ID 2JY6 onto each Ub unit. The UBQLN1 UBA exhibits 97% sequence identity with the UBQLN2 UBA domain. N-termini of each UBA domain are marked with ‘N’.

Table S1. K_d determined from NMR titration experiments.

	K_d (μM) [a]
^{15}N UBA with K48-Ub4	24.3 ± 8.0
^{15}N UBA with K63-Ub4	6.1 ± 1.8
^{15}N UBA with Ub	7.7 ± 0.9
^{15}N 450-624 with K11-Ub4	41.5 ± 11.6
^{15}N 450-624 with K63-Ub4	16.2 ± 8.9
^{15}N 450-624 with M1-Ub4	32.5 ± 7.2
^{15}N 450-624 with HOTag6-Ub	15.8 ± 4.6
^{15}N 450-624 with Ub	3.3 ± 1.0

[a] K_d was determined from the average K_d from ~10-12 residue-specific titration curves, and errors are the standard deviation of the K_d values over these titration curves.

Table S2. Structural parameters of polyUb from SAXS data analysis.

Samples	R_g (Å) [a] (Guinier)	R_g (Å) [b] (GNOM)	Dmax (Å) (GNOM)
K48-Ub4	25.67 ± 0.05	26.19 ± 0.07	97
K63-Ub4	32.40 ± 0.07	34.17 ± 0.14	133
M1-Ub4	32.42 ± 0.03	34.22 ± 0.21	140
HOTag6-G10-Ub	37.81 ± 0.06	39.06 ± 0.16	135

Indicated in parentheses are methods/software used for R_g analysis.

[a] The R_g and errors are determined from the linear fit of ln(I(q)) vs. q^2.

[b] The R_g and errors are determined from choosing multiple values of D_{max}.

Table S3. Summary of SV-AUC experiments with UBQLN2, Ub4 chains, and UBQLN2:Ub4 complexes.

Samples	s*, $s_{20,w}$ [a]	f/f_0 [b]	Loading Concentration (μM)	MSSV [c] Calculated Concentration (μM)	MSSV Calculated Stoichiometry of Complex
UBQLN2 487-624	1.23, 1.25	1.701	200	-	-
K48-Ub4	2.58, 2.64	1.346	100	-	-
K63-Ub4	2.49, 2.55	1.394	100	-	-
UBQLN2: K48-Ub4 complex [d]	2.8, 2.84	1.617	200 : 100 UBQLN2:Ub4	190.0 : 98.8 UBQLN2:Ub4	1.9:1
UBQLN2: K63-Ub4 complex [d]	2.7, 2.7	1.635	200 : 100 UBQLN2:Ub4	196.7 : 95.0 UBQLN2:Ub4	2.1:1

[a] Experimental sedimentation coefficients (s*) and standard sedimentation coefficients ($s_{20,w}$) after correcting for water at 20 °C.

[b] Frictional ratio.

[c] MSSV analysis was performed to determine protein concentrations in the complex and overall binding stoichiometry using parameters in Table S4 (see Methods).

[d] UBQLN2 here is UBQLN2 487-624, a construct previously shown to be monomeric (Dao et al., 2018).

Table S4. Parameters for MSSV analysis.

Samples	ε_k λ=260 (M^{-1} cm^{-1})	ε_k λ=280 (M^{-1} cm^{-1})	Ratio [a]
UBQLN2 487-624	5555	5500	1.01
K48-Ub4	9882	5960	1.66
K63-Ub4	10810	5960	1.81

[a] D_{norm} = 0.2730/0.2344 (values > 0.06 are considered good for spectral discrimination).

Table S5. SEC-MALS-SAXS Data Collection and Analysis.

(*a*) Sample details				
	1	2	3	4
Organism	*H. sapiens*	*H. sapiens*	*H. sapiens*	*H. sapiens*
Source (Catalogue No. or reference)	*Expressed in E. coli (this work)*	*Expressed in E. coli (this work)*	*Expressed in E. coli (this work)*	*Expressed in E. coli (this work)*
Description: sequence (including Uniprot ID + uncleaved tags), bound ligands/modifications, *etc.*	K48-Ub4 (distal Ub is K48R, all other Ub units are WT Ub)	K63-Ub4 (distal Ub is K63R, all other Ub units are WT Ub)	M1-Ub4 (linear tetraubiq.)	HOTag-G_{10}-Ub (see Methods)
Extinction coefficient ε in M^{-1} cm^{-1} (wavelength in nm)	5960 (280)	5960 (280)	5960 (280)	6990 (280)
Molecular mass *M* from chemical composition (Da)	34,200	34,200	34,200	13,200
For SEC-SAS, loading volume/concentration (mg ml^{-1}), injection volume (µl), flow rate (ml min^{-1})	7.0, 300, 0.6	7.0, 300, 0.6	7.0, 300, 0.6	4.5, 300, 0.6
Solvent composition and source	pH 6.8 20 mM NaPhos, 0.5 mM EDTA, 0.02% NaN_3	pH 6.8 20 mM NaPhos, 0.5 mM EDTA, 0.02% NaN_3	pH 6.8 20 mM NaPhos, 0.5 mM EDTA, 0.02% NaN_3	pH 6.8 20 mM NaPhos, 0.5 mM EDTA, 0.02% NaN_3

(*b*) SAS data collection parameters	
Source, instrument and description or reference	BioCAT facility at the Advanced Photon Source beamline 18ID with Pilatus3 X 1M (Dectris) detector
Wavelength (Å)	1.033
Beam geometry (size, sample-to-detector distance)	150 (h) x 25 (v) focused at the detector
Camera Length (m)	3.658
q-measurement range ($Å^{-1}$)	0.003-0.35
Absolute scaling method	Glassy Carbon, NIST SRM 3600
Basis for normalization to constant counts	To transmitted intensity by beam-stop counter
Method for monitoring radiation damage, X-ray dose where relevant	Automated frame-by-frame comparison of relevant regions using CORMAP (Franke et al., 2015) implemented in BioXTAS RAW
Exposure time, number of exposures	0.5 s exposure time with a 2 s total exposure period (0.5 s on, 1.5 s off) of entire SEC elution
Sample configuration including path length and flow rate where relevant	SEC-MALS-SAXS. Size separation used a Superdex 200 10/300 Increase column and a

	1260 Infinity II HPLC (Agilent Technologies). UV data was measured in the Agilent, and MALS-DLS-RI data by DAWN HELEOS-II (17 MALS + 1 DLS channels) and Optilab T-rEX (RI) instruments (Wyatt Technology). SAXS data was measured in a sheath-flow cell (Kirby et al., 2016), effective path length 0.542 mm.
Sample temperature (ºC)	20

(*c*) Software employed for SAXS data reduction, analysis and interpretation	
SAXS data reduction	Radial averaging; frame comparison, averaging, and subtraction done using BioXTAS RAW 2.1.1 (Hopkins et al., 2017)
Calculation of ε from sequence	ProtParam (ExPASy)
Basic analyses: Guinier, M.W., *P*(*r*), scattering particle volume (*e.g.* Porod volume V_P or volume of correlation V_c)	Guinier fit and M.W. using BioXTAS RAW, P(r) function using GNOM (Svergun, 1992). RAW uses MoW and Vc M.W. methods (Piiadov et al., 2019; Rambo and Tainer, 2013)
MALS-DLS-RI analysis	Astra 7 (Wyatt)

(*d*) Structural parameters				
Guinier Analysis	K48-Ub4	K63-Ub4	M1-Ub4	HOTag-Ub
$I(0)$ (cm^{-1})	0.0306 ± 0.00003	0.0326 ± 0.00004	0.02832 ± 0.00004	0.02688 ± 0.00006
R_g (Å)	25.67 ± 0.05	32.40 ± 0.07	32.42 ± 0.03	37.81 ± 0.06
q-range ($Å^{-1}$)	0.003 – 0.05127	0.003 – 0.04013	0.003 – 0.03984	0.00443 – 0.03556
Quality-of-fit parameter (with definition)	0.9943 (r^2)	0.9946 (r^2)	0.9920 (r^2)	0.9966 (r^2)
M from MALS (kDa)	33.7	34.5	33.9	53.4
P(*r*) analysis	K48-Ub4	K63-Ub4	M1-Ub4	HOTag-Ub
$I(0)$ (cm^{-1})	0.0306	0.0352	0.0286	0.0271
R_g (Å)	26.17	34.04	34.22	39.06
d_{max} (Å)	97	135	140	135
q-range ($Å^{-1}$)	0.003 – 0.3491	0.003 – 0.3491	0.003 – 0.03491	0.003 – 0.3491
Quality-of-fit parameter (with definition)	1.0441 (chi2)	1.0522 (chi2)	1.0373 (chi2)	1.0075 (chi2)

Supplementary Movie

Movie S1. UBQLN2 undergoes phase separation in the presence of Ub and K63-selective ubiquitination machinery, related to Fig. 6.

Time-lapse fluorescence microscopy monitoring UBQLN2 droplet formation in the presence of Ub and K63-selective ubiquitination machinery. Imaging was done in solution above the coverslip. Movie is about 31 minutes in real time. Initial experimental conditions: 50 μM Ub and UBQLN2, 30 nM Dylight 650-labeled UBQLN2, 1 μM mE1, 2 μM His-Mms2, 4 μM GST-Ubc13, 10 mM ATP and $MgCl_2$, 3 mM TCEP, 50 mM Tris pH8, 37 ºC. As time goes on, the amount of Ub in solution decreases while the amounts of different K63-linked polyUb chains increase.